1

Introduction

Hiroshi Ishikawa

1.1 Evolution of Optical Communication Systems and Device Technologies

Deployment of the optical communication systems started at the end of 1970s. The bit rate of the early-stage systems was 100 Mb/s (1980), increasing to 400 Mb/s, 565 Mb/s, 1.6 Gb/s, 2.4 Gb/s and 10 Gb/s over the past three decades. Increasing the transmission capacity was achieved not just by increasing the bit rates as wavelength division multiplexing (WDM) technology was developed in the 1990s. Systems capable of 100–200 wavelengths multiplexing with a single channel bit rate of 2.4 Gb/s and 10 Gb/s were deployed, having scalable total capacities up to 2 Tb/s. Recently, deployments of WDM systems with a single channel bit rate of 40 Gb/s have started. Looking into the future, we will be required to realize still larger capacity networks, as will be discussed later.

Owing to the above-mentioned increase in transmission capacity, broadband Internet network systems have come to be used widely since we entered Twenty-first century. Internet protocols (IP), various browsing technologies, varieties of related software, and increased performance of personal computers and routers, largely contributed to the spread of broadband networks, which have had a huge impact on our society and our daily life. Worldwide e-commerce and e-business has become an essential part of our economy with outsourcing of office jobs, research and development being done using networks. Even production at remote sites is becoming possible though networks. The world-wide impact of broadband networks is clearly described in such books as *Revolutionary Wealth* by Alvin Toffler and Heidi Toffler[1], and *The World is Flat* by Thomas L. Friedman[2].

When we looked back the technological evolution of these networks, development of new or higher performance devices and components played crucial roles. Such devices were low-loss optical fibers, semiconductor lasers, detectors such as APDs (avalanche photodiodes) and PIN photodiodes, integrated driver circuits, multiplexing and demultiplexing ICs, and fiber

Ultrafast All-Optical Signal Processing Devices Edited by Hiroshi Ishikawa

amplifiers. Many passive components such as arrayed waveguide gratings (AWG) and optical filters were needed for WDM systems.

We can see a good example in light sources showing how their innovation contributed to an increase in transmission bit rates. First, Fabry-Perot lasers, which lased in multiple spectra enabled transmission rates of up to 400 Mb/s. To increase the bit rate to more than 1 Gb/s, lasers with single wavelengths were essential to minimize the effect of chromatic dispersion of fiber. Distributed feedback (DFB) lasers were developed to this end. For longer-span transmission with bit rates above 10 Gb/s, wavelength chirp in a single lasing spectrum was a problem. Then the external modulation scheme was developed. Electro-optic modulators using $LiNbO_3$, semiconductor-based, electro-absorption modulators (EAM) were developed. Monolithic integration of DFB laser and EAM was done to realize a compact light source. Owing to these advances in light sources together with advances in other devices and technologies, it was possible to increase the transmission bit rate. If we target much higher bit rate systems, such as 100 Gb/s and 1 Tb/s, for future applications, the key will be the development of new and higher performance devices as well.

1.2 Increasing Communication Traffic and Power Consumption

Figure 1.1 shows the long term trend of communication traffic in JPIX, which is one of the major Internet exchangers in Tokyo. The traffic in JPIX is increasing by 40 to 50 % per year. Figure 1.2 shows the total traffic in Japan. The plots using closed circles are the time-averaged amount of information per second being downloaded from networks as announced by MIC (Ministry of Internal Affairs and Communications). The value was 324 Gb/s at November 2004. This increased to 722 Gbps in May 2007. The solid line in the figure is the estimated total traffic assuming a 40 % annual increase. One of the driving forces for this rapid increase is the increase in subscribers to broadband. Initially, ADSL (Asymmetrical Digital Subscriber Line) was used; however, recently the FTTH (Fiber to the Home) subscribers are increasing

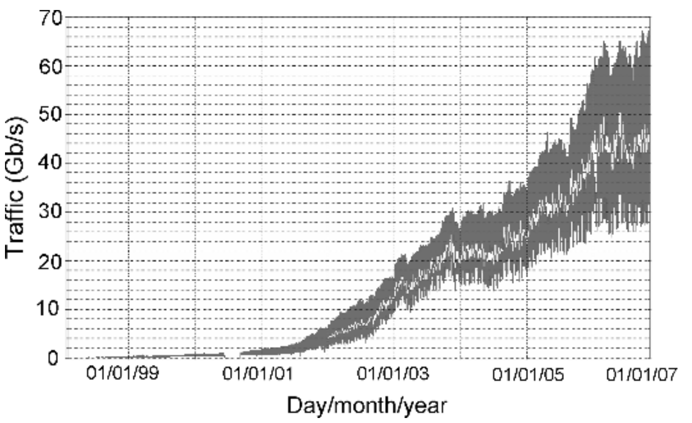

Figure 1.1 Internet traffic in JPIX, which is one of the major Internet exchangers in Tokyo. (Reproduced by permission of JPIX. (http://www/jpix.ad.jp/techncal/traffic.html))

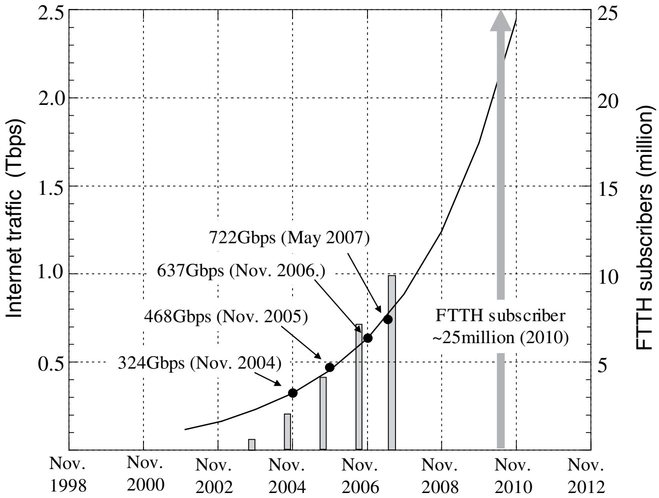

Figure 1.2 Total traffic in Japan. Solid circles are evaluated value by Ministry of Internal Affairs and Communications. The line is the fit assuming a 40 % annual increase. Bars show the subscribers to FTTH

rapidly. NTT, one of the major carrier companies in Japan, is aiming at 20 million subscribers to FTTH by 2010. The bars in Fig. 1.2 are subscribers to FTTH. NTT is to bring NGN (Next Generation Network) into service in 2008. NGN is an IP-based network enabling various services with higher quality [3].

The dramatic increase in traffic and the plan to increase various services will cause a serious problem, namely the power consumption of the network equipment. Figure 1.3 shows the router power consumption in Japan as estimated by T. Hasama of AIST (National Institute of Advanced Industrial Science and Technology). The power consumption in 2001 is based on actual data. Assuming a 40 % annual increase in traffic and reduction of the CMOS-LSI drive voltage, plotted as closed circles in the figure, the power consumption of routers will reach 6.4 % of the total power generation in 2020 even for the low CMOS-LSI drive voltage of 0.8 V. If the drive voltage reduction of CMOS-LSI is insufficient, the power consumption will still easily reach a few tens of a percentage point or more. This means we cannot have the benefits of larger capacity networks.

One of the causes of large power consumption in the present network is the WDM scheme and electrical routing of the packet signals. The WDM requires O/E (optical to electrical) signal and E/O (electrical to optical) signal conversion circuits with the same number as that of the wavelength, resulting in an increase in power consumption. In addition to this, electrical signal processing for IP packet routing and switching at the router consumes large amounts of power. If we could realize 100 Gb/s to 1 Tb/s bit-rate transmission, huge capacity data could be transmitted with a small number of wavelengths, which might reduce the power consumption. If we could process ultrafast signals without converting to electrical signals, this would also reduce the power consumption of routers. Consequently, the development of ultrafast all-optical devices is very important for future, low power-consumption huge capacity networks

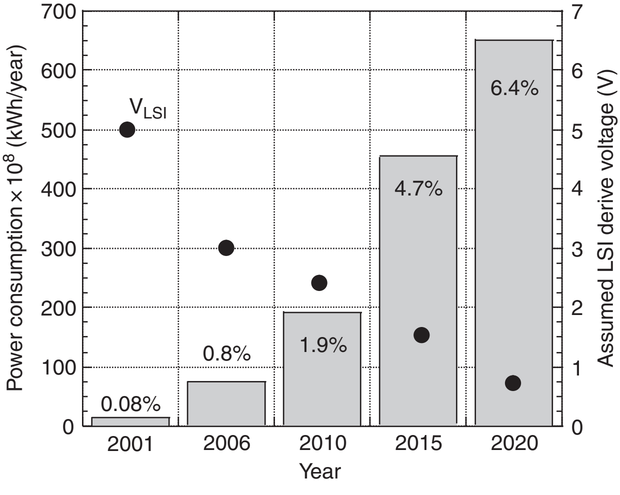

Figure 1.3 Estimated power consumption by Internet routers in Japan. Original data is from T. Hasama of AIST. The value for 2001 is actual data. Plots shown by solid circles are the assumed drive of LSI voltage used in routers. The percentages in the figure are the proportion of total power generation. If we assume a 40 % increase in traffic, the router power consumption reaches 6.4 % of the total power generation in 2020 even for a low LSI drive voltage of 0.8 V

1.3 Future Networks and Technologies

1.3.1 Future Networks

Forecasting the future of networking is of large importance in planning research and development. It is obvious that the traffic of video content will keep on increasing. At present, a large proportion of the network bandwidth is occupied by video content, such as TV and movies, and moving-picture distribution services. The convergence of broadcasting and communication will soon take place in NGN (Next Generation Network). Network users will require higher resolution pictures; however there is a limitation on resolution due to the limited bandwidth. International distribution of 4K-digital cinema (for resolution of 2000×4000, the required bandwidth is above 6 Gb/s without compression) by network was demonstrated using data compression by JPEG2000 [4]. NHK (the Japanese public broadcasting organization) is developing ultra-HDTV (high definition TV) having a resolution of 4320×7680, requiring a bandwidth of 72 Gb/s, and is planing to start broadcasting ultra-HDTV in 2025 [5].

If we could get rid of the bandwidth limitation, there would arise a lot of new applications. Higher resolution, real-time, moving pictures with realistic sound will make the TV conference a far more useful tool. International conferences could even be held using remote-presence technology. This would reduce the energy consumption by reducing the traffic. Medical applications for the network will also be important. Using high-resolution pictures without time delay, remote diagnosis can be done, and even remote surgery is within its scope. Other important associated technology would be grid technology. One of the present applications of grid technology is to establish connections or paths between various computer sites or data storages. The large bandwidth optical paths, which can be controlled by a user, will enable high performance grid computing (e-science) by connecting computers worldwide. Grid-based virtual huge capacity storage, and grid-based economy (e-economy, e-commerce, e-production) will also be important issues.

When we look at the current IP-based network, it is not suited to handling such a huge capacity of data. It is optimized rather to low granularity traffic and requires data compression for large-capacity data because of the bandwidth limitation. This causes the time delay, and we cannot obtain the benefit of real-time information. A novel network capable of real-time, high-capacity, transmission is required. One candidate is the optical-path network, in which end-to-end connection and broadcasting end to multi-ends connection can be achieved with optical paths where large-scale optical switches are used for routing. The concept of optical path has been discussed in terms of wavelength path or virtual wavelength path [6]. The dynamic huge-scale path network including the wavelength path with very high bit rate is highly attractive as a future network for huge capacity data transmission. In such path systems, information can be transmitted transparently, i.e. regardless of the modulation format and bit rate, without using electronic routers. Combination of IP based networks, which handle small granularity data, and dynamic optical path networks, which handle huge capacity data with very high bit rates, is one of the promising forms of the future network.

1.3.2 Schemes for Huge Capacity Transmission

There are two ways of achieving huge capacity transmission. One is the optical time division multiplexing (OTDM) technology as illustrated in Figure 1.4, and the other is the employment of multilevel modulation schemes as illustrated by Figure 1.5.

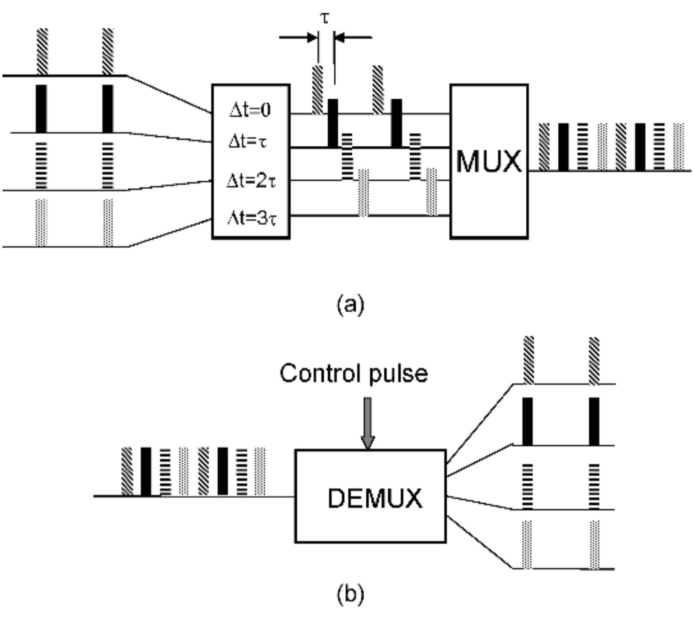

Figure 1.4 Optical time division multiplexing (OTDM) scheme. (a) By giving proper delay to each channel we can generate a very fast optical signal. (b) For demultiplexing we are required to develop all-optical switches

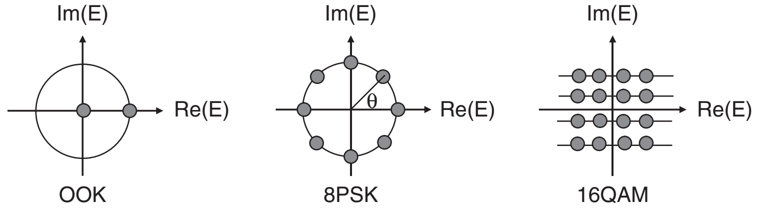

Figure 1.5 Constellation diagram of OOK (on–off keying), 8 PSK (phase shift keying) and 16 (quadrature amplitude modulation). By utilizing phases of light waves we can realize multilevel modulation

In the OTDM scheme, optical signals from different channels are multiplexed by applying a proper delay to each channel in order to get high bit-rate signals. We can generate high bit rates, for example 160 Gb/s or 1.28 Tb/s [7], which cannot be achieved by electric circuits. To make the OTDM systems into real ones, we need to develop ultrafast, all-optical signal processing devices. There are ultrafast light sources and ultrafast all-optical gate switches for such functions as gating, clock extraction, 2R (retiming and reshaping) operations, and DEMUX (demultiplexing). To make the system flexible, a wavelength conversion device is also essential. Dispersion compensation including polarization-mode dispersion, is also an important issue for long-distance transmission.

The other scheme involves the use of multilevel modulation, which not only uses the amplitude of light but also the phase [8, 9]. By utilizing phases of the light field we can perform multilevel modulation. Figure 1.5 shows examples of multilevel modulation in the form of constellation mapping. The horizontal axis is the real part of the electric field and the vertical axis is the imaginary part. Figure 1.5(a) is the conventional on–off keying (OOK). Figure 1.5(b) is 8 PSK (phase shift keying), which can transmit 3 bit/symbol, and (c) is 16 QAM (quadrature amplitude modulation) capable of 4 bit/symbol modulation. Precise control of phases and sophisticated decoding technology are required to realize a large multilevel [10, 11]. The multilevel scheme has an advantage in that it can increase the total capacity without increasing the symbol rate. This makes the dispersion compensation easier.

1.4 Ultrafast All-Optical Signal Processing Devices

1.4.1 Challenges

In this book we describe the challenges for semiconductor-based ultrafast (100 Gb/s - 1 Tb/s) all-optical signal processing devices. A major application is in ultrafast OTDM networks; however, a multi-level scheme based on a symbol rate beyond 100 Gb/s could also be a possibility in further increasing the transmission rate. Focus is put on semiconductor-based devices, although fiber-based devices are used for ultrafast OTDM experiments, for example, NOLM (Nonlinear Optical Loop Mirror) [12, 13]. Advantages of semiconductor devices when compared with fiber devices are their small size and possible integration of devices for higher functionality. With semiconductor devices, however, there is a lot of difficulties in realizing practical devices. One of the major difficulties is the intrinsic one that faster all-optical device operation based on optical nonlinearity requires larger optical energy. This is theoretically illustrated in the next section. This problem can be avoided in fiber devices because long fiber-lengths can be used to obtain sufficient nonlinearity for low energy operation. In semiconductor devices, although the nonlinear susceptibility is greater than with optical fibers, device sizes are very small. It is not, therefore, easy to realize low-energy operating devices; hence, for the development of ultrafast all-optical semiconductor devices, full utilization of many new ideas and concepts are required.

A systematic challenge for semiconductor-based, ultrafast all-optical devices was The Femtosecond Technology Project (1995–2004) in Japan, which was conducted with the support of the Ministry of Trade and Industry, and NEDO (New Energy and Industrial Technology Development Organization) [14]. Mode-locked semiconductor lasers were developed, as were various types of all-optical gate switches, and WDM transmission technology based on 160 Gb/s–320 Gb/s OTDM signals. Described in this book are mode-locked lasers (Chapter 2), symmetric Mach–Zehnder gate switch (Chapter 3), intersub-band transition gate switches (Chapter 5), four-wave mixing wavelength converters (Chapter 6), and transmission technologies (Chapter 7). Another project, named 'Research and Development on Ultrahigh-speed Backbone Photonic Network Technologies' (1996–2005) was conducted under the auspices of NICT (National Institute of Information and Communication Technology). In this project, a 160-Gb/s CS-RZ (carrier suppressed return to zero) signal was generated by OTDM technology using an electro-absorption modulator (EAM) [15]. A field transmission experiment was demonstrated over 635 km. The OTDM light source developed in this project is described in Chapter 2, and the transmission experiment is briefly reviewed in Chapter 7. Outside of these projects, much interesting research work has been done worldwide, including a device using an ultrafast photodiode and traveling-wave electro-absorption modulator, described in Chapter 4, and a use of SOA with wavelength filter enabling use of only the very fast response component of SOA response (Chapter 3).

1.4.2 Basics of the Nonlinear Optical Process

For ultrafast, all-optical, signal processing using semiconductor-based devices, we use optical nonlinear effects, mainly the third-order nonlinearity. The third-order process is highly useful since it gives such effects as absorption saturation (gain saturation) and four-wave mixing. Here we briefly look at the third-order nonlinear process, taking the simplest two-level system as an example in order to achieve basic understanding of the device operation and to illustrate the intrinsic difficulty with all-optical ultrafast devices.

Figure 1.6 shows a two-level system. We assume N two-level systems with inversion symmetry in a volume V. We consider a case where only one frequency plane wave with angular frequency ω is applied. The response of the two-level system to the optical field can be described by a density matrix equation of motion [18, 19]. If we write down all the components of the equation of motion:

$$\frac{d}{dt}\rho_{aa} = \frac{i}{\hbar}(\rho_{ab}H_{ba} - H_{ab}\rho_{ba}) - \gamma_a\left(\rho_{aa} - \rho_{aa}^{(0)}\right) \tag{1.1}$$

$$\frac{d}{dt}\rho_{bb} = \frac{i}{\hbar}(\rho_{ba}H_{ab} - H_{ba}\rho_{ab}) - \gamma_b\left(\rho_{bb} - \rho_{bb}^{(0)}\right) \tag{1.2}$$

$$\frac{d}{dt}\rho_{ab} = \frac{i}{\hbar}(E_b - E_a)\rho_{ab} + \frac{i}{\hbar}(H_{ab}\rho_{aa} - H_{ab}\rho_{bb}) - \gamma_{ab}\rho_{ab} \tag{1.3}$$

$$\frac{d}{dt}\rho_{ba} = \frac{i}{\hbar}(E_a - E_b)\rho_{ba} + \frac{i}{\hbar}(H_{ba}\rho_{bb} - H_{ba}\rho_{aa}) - \gamma_{ab}\rho_{ba} \tag{1.4}$$

For a plane-wave electric field $\mathbf{E}\,(\omega)$, the perturbation Hamiltonian under dipole approximation can be written as,

$$H_{ab}\,(\omega) = -\boldsymbol{\mu}_{ab} \cdot \mathbf{E}\,(\omega) = -\boldsymbol{\mu}_{ab} \cdot (\mathbf{E}_{\omega} e^{-i\omega t} + c.c.) \tag{1.5}$$

where $\boldsymbol{\mu}_{ab}$ is a dipole moment given by:

$$\boldsymbol{\mu}_{ab} = \langle a|e\mathbf{r}|b\rangle \tag{1.6}$$

$\rho_{aa}^{(0)}$ and $\rho_{bb}^{(0)}$ are the unperturbed diagonal elements of the density matrix, which can be replaced by electron distribution functions such as Fermi–Dirac or Boltzmann distribution function under thermal equilibrium. γ_a and γ_b are the phenomenological relaxation rates of the diagonal component of the thermal equilibrium. We may put $\gamma = \gamma_a = \gamma_b = 1/T_1$, where T_1 is the energy relaxation time of an electron. γ_{ab} is the dephasing rate of the off-diagonal element. Elastic scattering, as well as inelastic scattering, of electrons contributes to the dephasing of a dipole. Its inverse is the dephasing time T_2.

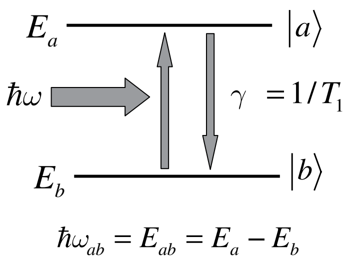

Figure 1.6 A model of two-level system

The equation of motion can be solved by using the iterative procedure. A first-order solution for the off-diagonal component can be obtained by using unperturbed diagonal terms for the right-hand side of Equation (1.3). Retaining only the resonant term, we obtain:

$$\rho_{ab}^{(1)}\,(\omega) = -\frac{\boldsymbol{\mu}_{ab} \cdot \mathbf{E}_{\omega} e^{-i\omega t}}{\hbar(\omega_{ab} - \omega) - i\hbar\gamma_{ab}}(\rho_{aa}^{(0)} - \rho_{bb}^{(0)}) + \text{cc.} \tag{1.7}$$

Inserting this into Equations (1.1) and , we obtain second-order solution, $\rho_{aa}^{(2)}$ and $\rho_{bb}^{(2)}$. Again, by inserting second-order diagonal terms into Equation (1.3), we obtain the third-order solution of the off-diagonal term. This is a rather tedious calculation procedure. Retaining only the resonant terms makes the analysis simpler. Once the density matrix components are known, the polarization of the system is given by:

$$\mathbf{P}\,(\omega) = \frac{2N}{V} Tr\,(\boldsymbol{\mu}\rho) = \frac{2N}{V}\,(\boldsymbol{\mu}_{ab}\rho_{ab} + \boldsymbol{\mu}_{ba}\rho_{ba}) \tag{1.8}$$

The first-order solution of the off-diagonal terms gives the first-order polarization, and the third-order off-diagonal terms give the third-order polarization. Retaining the first- to the third-order terms, the generated polarization can be written as:

$$\mathbf{P}(\omega) = \varepsilon_0 \left(\chi^{(1)}(\omega) + \chi^{(3)}(\omega)\,|\mathbf{E}_\omega|^2\right)\mathbf{E}_\omega \tag{1.9}$$

where ε_0 is the vacuum dielectric constant, $\chi^{(1)}$ is linear susceptibility and $\chi^{(3)}$ is the third-order nonlinear susceptibility. There is no second-order nonlinearity because we have assumed a system with inversion symmetry. The above iterative solutions of the equation of motion give susceptibilities as:

$$\chi^{(1)}(\omega) = -\frac{2N|\mu_{ab}|^2}{\varepsilon_0 V}\frac{1}{\hbar(\omega_{ab}-\omega) - i\hbar\gamma_{ab}}(\rho_{aa}^{(0)} - \rho_{bb}^{(0)}) \tag{1.10}$$

$$\chi^{(3)}(\omega) = -\frac{8N|\mu_{ab}|^4\gamma_{ab}(\rho_{aa}^{(0)} - \rho_{bb}^{(0)})}{\varepsilon_0 V\gamma\,(\hbar\omega - \hbar\omega_{ab} + i\hbar\gamma_{ab})\left(\hbar^2(\omega_{ab}-\omega)^2 + \hbar^2\gamma_{ab}^2\right)} \tag{1.11}$$

Development of a light electric field under nonlinear susceptibility can be written using slowly varying envelope approximation as:

$$\frac{d}{dz}\mathbf{E}_\omega = -\frac{1}{2ik}\left(\varepsilon_0\mu_0\omega^2 + \varepsilon_0\mu_0\omega_p^2\chi^{(1)} - k^2\right)\mathbf{E}_\omega - \frac{1}{2ik}\varepsilon_0\mu_0\omega^2\chi^{(3)}|\mathbf{E}_\omega|^2\mathbf{E}_\omega \tag{1.12}$$

where μ_0 is the vacuum permeability. This can be rewritten by separating the real and imaginary part of the susceptibility as:

$$\frac{d}{dz}\mathbf{E}_\omega = \frac{i}{2k}\varepsilon_0\mu_0\omega^2\left[1 + \chi_R^{(1)} + \chi_R^{(3)}\,|E_\omega|^2 - \frac{k^2}{\varepsilon_0\mu_0\omega^2}\right]\mathbf{E}_\omega - \frac{1}{2k}\mu_0\varepsilon_0\omega^2\left(\chi_I^{(1)} + \chi_I^{(3)}\,|\mathbf{E}_\omega|^2\right)\mathbf{E}_\omega \tag{1.13}$$

Suffix R denotes the real part, and I denotes the imaginary part. For this equation to hold:

$$k^2 = \varepsilon_0\mu_0\omega^2\left(1 + \chi_R^{(1)} + \chi_R^{(3)}\,|\mathbf{E}_\omega|^2\right) \tag{1.14}$$

$$\frac{d}{dz}\mathbf{E}_\omega = -\frac{\omega}{2cn}\left(\chi_I^{(1)} + \chi_I^{(3)}\,|\mathbf{E}_\omega|^2\right)\mathbf{E}_\omega \tag{1.15}$$

Equation (1.14) gives the refractive index as:

$$n = \left(1 + \chi_R^{(1)} + \chi_R^{(3)}\,|\mathbf{E}_\omega|^2\right)^{1/2} \tag{1.16}$$

This equation means that the refractive index changes in the optical field through a third-order nonlinear process. Equation (1.15) can be rewritten as an equation describing optical power propagation. Using:

$$\frac{d}{dz}\,|\mathbf{E}_\omega|^2 = \mathbf{E}_\omega^*\frac{d\mathbf{E}_\omega}{dz} + E\frac{d\mathbf{E}_\omega^*}{dz} \tag{1.17}$$

$$|\mathbf{E}_\omega|^2 = \frac{2Z_0}{n}P \tag{1.18}$$

where P is the optical power density and Z_0 is the vacuum impedance given by:

$$Z_0 = \sqrt{\frac{\mu_0}{\varepsilon_0}} \tag{1.19}$$

We can obtain the equation for the optical power density as:

$$\frac{dP}{dz} = -\frac{\alpha_0 P}{1 - \frac{Z_0 \chi_I^{(3)}}{2n\chi_I^{(1)}}} = -\frac{\alpha_0 P}{1 + \frac{P}{P_s}} \tag{1.20}$$

where α_0 is the linear absorption coefficient and is expressed as:

$$\alpha_0 = \frac{\omega}{cn}\chi_I^{(1)} = \left(\frac{2N}{V}\right)\frac{Z_0\omega\mu_{ab}^2}{n}\frac{\hbar\gamma_{ab}}{\hbar^2(\omega_{ab}-\omega)^2 + \hbar^2\gamma_{ab}^2}\Delta\rho^{(0)} \tag{1.21}$$

where $\Delta\rho^{(0)} = \rho_{bb}^{(0)} - \rho_{aa}^{(0)}$ and P_s is:

$$P_s(\omega) = -\frac{2n\chi_I^{(1)}}{Z_0\chi_I^{(3)}} = \frac{cn\varepsilon_0\gamma}{2\mu_{ab}^2\gamma_{ab}}\left(\hbar^2(\omega_{ab}-\omega)^2 + \hbar^2\gamma_{ab}^2\right) \tag{1.22}$$

Equation (1.20) means that the absorption coefficient is reduced for large optical power density and is half of the initial value for $P = P_s$. P_s is called the saturation power density and we can use this for an all-optical gate. If we introduce an intense control pulse to the two-level system, the system becomes transparent by absorption saturation. Under this condition, a weak signal light can pass through the two-level system. This is the 'on state' of the gate. When we turn off the control pulse, the system is again absorptive with a time constant of T_1, and the gate switch is in the 'off-state'. It can be seen that the absorption saturation takes place over the homogenous width of $\Delta\omega = \omega - \omega_{ab} = \hbar\gamma_{ab}$. When there is population inversion, the two-level system has optical gain, and the third order process gives the gain saturation. SOA corresponds to this case. This also can be used as an all-optical gate switch.

To examine the relationship between the response speed and the optical power density needed to saturate the two-level system, we consider the on resonant case, i.e. $\omega = \omega_{ab}$. The saturation power density is given by:

$$P_s = \frac{n\hbar^2\gamma\gamma_{ab}}{2\mu_{ab}^2 Z_0} = \frac{cn\varepsilon_0\hbar^2}{2\mu_{ab}^2 T_1 T_2} \tag{1.23}$$

The smaller T_1 and T_2 give faster response speeds while, however, smaller T_1 and T_2 give larger P_s. Large optical energy is needed for a very fast nonlinear response. This is the intrinsic limitation in using nonlinearity for all-optical signal processing devices. In the evaluation of ultrafast devices, we use short pulses. It is customary to use pulse energy rather than optical power density as a measure of device performance. The saturation pulse energy is the product of P_s, the cross section of the beam, and the pulse width. The discussion on the relationship between the response speed and optical power density (pulse energy) also holds for the refractive index, because of Kramers–Kronig relation that connects the absorption coefficient and refractive index.

More detailed analysis reveals that there are varieties of interesting effects in the optical nonlinearity. For example, if we assume pump wave ω_p and signal wave ω_s of different frequencies and consider beat frequency $2\omega_p - \omega_s$, we obtain the third-order susceptibility for nondegenerate four-wave mixing. This frequency is the beat frequency between $\omega_p - \omega_s$ and ω_p, i.e. the pump wave ω_p is scattered by the beat frequency $\omega_p - \omega_s$ to generate a new frequency $2\omega_p - \omega_s$. Detailed discussion on four-wave mixing in SOA is described in Chapter 6, which considers some other effects on the third-order nonlinear susceptibility. If we further extend the analysis to multi-level systems, we obtain expressions for multi-photon absorption and Raman scattering processes [17].

To extend the analysis from the simple two-level system to semiconductor band structures, following substitution using the wave number of electrons, **k** applies.

$$\left(\frac{2N}{V}\right) \rightarrow D(\mathbf{k})\, d\mathbf{k}, \text{ where } D(\mathbf{k}) \text{ is the density of state.}$$

Express parameters in terms of **k**, for example $\hbar\omega_i \rightarrow \frac{\hbar^2 \mathbf{k}_i^2}{2m^*}$, where m^* is the electron effective mass:

$$\rho_{aa}^{(0)}, \rho_{bb}^{(0)} \rightarrow \text{Fermi–Dirac distribution function expressed in terms of } \mathbf{k}$$

Then integrate over **k**. This gives the parameters for semiconductor-based systems. It goes without saying that relationship (1.23) also holds for semiconductors.

1.5 Overview of the Devices and Their Concepts

Here we briefly review the devices described in this book in order to have an overview of their basic concepts as related to ultrafast operation. Lots of new ideas are employed and new challenges have arisen.

In Chapter 2, we describe ultrafast light sources. These are mode-lock lasers and EAM-based light sources. The mode-locked laser uses the absorption-saturation effect for mode locking. Hybrid mode locking using microwave modulation and sub-harmonic synchronous locking were employed to generate high repletion rate short pulses with small jitter. Mode-locked lasers can also be used for clock extraction from the deteriorated received signal. The 3R (retiming, retiming, regeneration) operation for a 160-Gb/s signal was demonstrated using mode-locked lasers. Also described in Chapter 2 is the EAM-based ultrafast light source. By cascading two EAMs, which are modulated by a 40-Gb/s electric signal, 3-ps width short pulses with 40 Gb/s repletion were generated. Then, a 160 Gb/s optical signal was generated by OTDM, i.e. by applying a proper time delay to four 40-Gb/s channels using space optics. An interesting point was that the CS-RZ (carrier suppressed return to zero) signal at 160 Gb/s was generated by controlling the phases of each channel by temperature. The CS-RZ modulation format is robust to nonlinear effect in the fiber, such as four-wave mixing, because of no carrier in the spectrum.

In Chapter 3, switching using a SOA (semiconductor optical amplifier) is discussed. In the SOA, population inversion is realized by current injection. When we put in an intense gate pulse, it causes a gain reduction and an associated refractive index change takes place. This is the third-order nonlinear process, and its basic principle can be understood by replacing the absorption coefficient in Equation (1.20) by the gain of SOA. A characteristic feature of this response is that it is very fast for the rise time; however, there is a slow component of the order of 1ns in the response recovery, which is the band-to-band recombination lifetime. This slow component has been the obstacle in realizing ultrafast switching devices above 100 Gb/s. Two methods are described for solving this problem. One is to use a wavelength filter to select only the very fast, blue-shifted component of the response [16, 17]. By using only the fast component, which is due to intraband electron–phonon scattering, we can perform wavelength conversion, 2R (retiming and reshaping) operation and DEMUX operation. Another method is to use the Symmetric Mach-Zehnder (SMZ) interferometer configuration. By putting SOA symmetrically at both arms of a SMZ, we can cancel out the slow response component by using gate on pulse and off pulse. Using the SMZ configuration, DEMUX operation of 640 Gb/s to 10 Gb/s was demonstrated. Error free DEMUX operations of 320 to 40 Gb/s and to 10 Gb/s were also demonstrated. Also demonstrated were the wavelength conversion and retiming and reshaping (2R) operations. It is interesting that this SMZ gate switch can be used for rather slow signal processing. Bit rate free 2R operation (2.5–42 Gb/s) was demonstrated for NRZ signals.

Chapter 4 describes a different approach to realizing ultrafast signal processing. The Uni-Traveling-Carrier Photodiode (UTC-PD), which has a very fast response with high output current, followed by a monolithically integrated traveling-wave electro-absorption modulator (TW-EAM), was used for ultrafast signal processing. In this method, very short gate pulses are converted to the electrical signal using UTC-PD, which has a 3-dB cut-off frequency of above 300 GHz. The electric signal modulates the optical signal by TW-EAM, which is monolithically integrated with the UTC-PD. Using this method, DEMUX operation of 320 Gb/s to 10 Gb/s was demonstrated. We are not bothered by the intrinsic relationship of response time and energy requirement inherent to the third-order nonlinear process. Careful design taking into account RC limit and phase matching of the traveling wave EAM modulator are crucial issues.

Chapter 5 describes the inter-sub-band transition (ISBT) gate. The ISBT gate utilizes the absorption saturation in the inter-sub-band transition in the conduction band of a very thin quantum well. To obtain a 1.55 μm transition, a deep potential well and ultra-thin well have to be employed. Material systems satisfying this are (GaN)/AlN, (CdS/ZnSe)/BeTe, and (InGaAs)/AlAs/AlAsSb material systems. Materials in parentheses are well layer materials. Response time depends on T_1 and T_2 times, which depend on parameters such as LO-Phonon energy, effective mass, and dielectric constant. Because of these parameters the (GaN)/AlN quantum well shows the fastest response, then (CdS/ZnSe)/BeTe, with the (InGaAs)/AlAs/AlAsSb system being the slowest. However, even in the slowest case, the response time is about 1 ps. Owing to the very fast response time of ISBT, we can realize a very fast absorption saturation type gate. A problem, however, is that gating energy becomes large for a fast response, as can be seen from Equation (1.23). Then in ISBT gates, much effort has been put into realizing low-gating energy despite the very fast response. In addition to the intensity gate based on absorption saturation, a new very interesting phenomenon has been found in the InGaAs/AlAs/AlAsSb ISBT gate, i.e all-optical, deep-phase modulation can be used on the loss-less TE mode probe light when the quantum well is illuminated by a TM gate pulse. This new phenomenon is quite useful, and wavelength conversion of picosecond pulses with 10 Gb/s repetition was demonstrated using this effect.

In Chapter 6, four-wave mixing (FWM) wavelength conversion using SOA is presented. Various methods of wavelength conversion are reviewed and then the chapter focuses on FWM using the semiconductor gain medium, SOA and semiconductor lasers. Various effects giving third-order nonlinear susceptibility are discussed. These are carrier density pulsation, carrier heating, and spectral hole burning. An impeding effect for the application of FWM for practical systems is the asymmetry in the wavelength conversion efficiency with respect to the pumping wavelength. The wavelength conversion efficiency from long wavelength to short wavelength is high, while the short to long is small. To solve this problem, quantum dot SOA was used, and almost symmetric wavelength conversion was demonstrated at 1.3 μm. The wavelength conversion of a 160-Gb/s signal was demonstrated at 1.55 μm, although there remained asymmetry. Also demonstrated was the use of a two-wave pumping scheme using bulk active layer SOA monolithically integrated with Mach–Zehnder interferometer configuration. This generates a replica of the signal at a different wavelength. Use of the conjugate wave for the compensation of the dispersion effect was also demonstrated using FWM.

In Chapter 7, transmission experiments performed using the devices illustrated in this book are reviewed. A 160-Gb/s based eight wavelength WDM experiment and a 320-Gb/s based ten wavelength WDM experiment were performed using mode-locked lasers (see Chapter 2) and SMZ gate switch (see Chapter 3). Another was a field experiment using an EAM-based CS-RZ light source (Chapter 2). In addition to these experiments, several recent experiments above 160 Gb/s are reviewed briefly, and the trends in very high bit rate transmission technologies are discussed. Based on these discussions and the state-of-the-art development of the devices described in this book, the technical issues to be overcome to make these devices useful and practical ones are discussed.

1.6 Summary

We saw that the development of new and higher performance devices has played a crucial role in higher bit rate systems. The increased communication capacity has brought us to a new era of the information society, where broadband Internet has had a huge impact on our daily life. We have the benefit of networks; however, we are facing the problem of increased power consumption by the network equipment. To take full advantage of the communications network we are required to establish new technologies that enable transmission of huge capacity data with minimum power consumption. One of the ways to achieve this is to introduce ultrafast, all-optical, signal processing. With ultrafast all-optical signal processing, we will be able to transmit huge amounts of data by OTDM by combining WDM and/or a multilevel scheme. To this end, semiconductor-based, ultrafast, all-optical signal processing devices are essential. There is a lot of difficulty in realizing satisfactory performances. We have discussed a third-order nonlinear process taking the simplest case, and showed that there is a restrictive relationship between the device response speed and the optical energy need for operation. In this book, readers will find a lot of new ideas and trials so far encountered in attaining our goal.

References

[1] A. Toffler and H. Toffler, *Revolutionary Wealth*, Alfred A. Knopf, NewYork, 2006.

[2] T. L. Friedman, *The World is Flat*, Farrar, Straus and Girnux, New York, 2005.

[3] A. R. Modarressi and S. Mohan, 'Control and management in next-generation networks: challenges and opportunities', *Communication Magazine, IEEE*, **43** (10), 94–102 (2000).

[4] T. Shimizu, D. Shirai, H. Takahashi, T. Murooka, K. Obana, Y. Tonomura, T. Inoue, T. Yamaguchi, T. Fujii, N. Ohta, S. Ono, T. Aoyama, L. Herr, N. van Osdol, X, Wang, M. D. Brown, T. A. DeFanti, R. Feld, J. Balser,

S. Morris, T. Henthorn, G. Dawe, P. Otto, and L. Smarr, 'International real-time streaming of 4K digital cinema', *Future Generation Computer Systems*, **22**, 929–939 (2006).
[5] Y. Fujita, 'Future networked broadcasting systems with ultrahigh-speed optic transmission technologies', *The Third International Symposium on Ultrafast Photonic Technologies*, Boston, August 2007.
[6] N. Nagatsu, S. Okamoto, K. Sato, 'Large scale photonic transport network design based on optical paths', *Proceedings: Global Telecommunications Conference*, Vol. 1, pp.321–327, London, 1996.
[7] M. Nakazawa, T. Yamamoto, and K. R. Tamura, '1.28 Tbit/s-70 km OTDM transmission using third- and fourth-order simultaneous dispersion compensation with a phase modulator', *Electron. Letters*, **36**, 2027–2029 (2000).
[8] T. Tokle, M. Serbay, J. B. Jensen, Y. Geng, W. Rosenkranz, and P. Jeppesen, 'Investigation of multilevel phase and amplitude modulation formats in combination with polarization multiplexing up to 240Gb/s', *IEEE Photon. Technology. Letters*, **18**, 2090–2092 (2006).
[9] K. Sekine, N. Kikuchi, S. Sasaki, S. Hayase, C. Hasegawa, and T. Sugawara, '40Gb/s, 16-ary (4 bit/symbol) optical modulation/demodulation scheme', *Electron. Letters*, **41**, 430–432 (2005).
[10] M. Nakazawa, M. Yoshida, K. Kasai, and J. Hongou, '20 Msymbol/s 64 and 128 QAM coherent optical transmission over 525 km using heterodyne detection with frequency-stabilized laser', *Electron. Letters*, **42**, 710–712 (2006).
[11] K. Kikuchi, 'Phase-diversity homodyne detection of multilevel optical modulation with digital carrier phase estimation', *IEEE Journal on Selected Topics in Quantum Electronics*, **12**, 563–570 (2006).
[12] N. J. Doran, and D. Wood, 'Nonlinear-optical loop mirror', *Optics Letters*, **13**, 56–58 (1988).
[13] T. Yamamoto, E. Yoshida, and M. Nakazawa, 'Ultrafast nonlinear optical loop mirror for demultiplexing 640 Gb/s TDM signals', *Electron. Letters*, **34**, 1013–1014 (1998).
[14] T. Sakurai, 'Ultrafast Photonic Device Technology in FST Project', *Europe–US–Japan Symposium on Ultrafast Photonic Technology*, Chiba, Japan, 2003.
[15] H. Murai, 'EA modulator based OTDM technique for 160 Gb/s optical signal transmission', *Journal of the National Institute of Information and Communication Technology*, **53**(2), 27–35 (2006).
[16] M. L. Nielsen, B. Lavigne, and B. Dagens, 'Polarity-preserving SOA-based wavelength conversion at 40 Gb/s using bandpass filtering', *Electron. Letters*, **39**, 1334–1335 (2003).
[17] Y. Liu, E. Tangdiongga, Z. Li, S. Zhang, H. de Waardt, G. D. Khoe, and H. J. S. Dorren, '80 Gb/s wavelength conversion using a semiconductor optical amplifier and an optical bandpass filter', *Electron. Lett*ers, **41**, 487–489 (2005).
[18] W. E. Lamb, 'Theory of an optical maser', *Phys. Rev.***134**, A1429–A1450 (1964).
[19] Y. R. Shen, *The Principle of Nonlinear Optics*, John Wiley & Sons, Inc. Hoboken, New Jersey, 2003.